IMPACT MELT SHEETS IN LUNAR BASINS: ESTIMATING THICKNESS FROM COOLING BEHAVIOR. Lionel Wilson[1] and James W. Head[2], [1]Lancaster Environment Centre, Lancaster University, LA1 4YQ, UK (l.wilson@lancaster.ac.uk); [2]Dept. Geological Sciences, Brown University, Providence, RI 02912.

Introduction: Impact melt deposits occur on the floors, walls and rims of lunar impact craters and basins [1, 2] and there is a range of field and experimental evidence that proportionally more melt is produced as a function of increasing crater size [3, 4]. Recent hydrocode models predict that basin-scale impacts will produce huge quantities of impact melt [5, 6]. The nature of impact melt formation and evolution in lunar basins is uncertain, however, due to post-basin flooding and modification by mare volcanic deposits, and obscuration of the basin interior [7] where the majority of melt resides [1, 2]. The Orientale basin [8-11] (Fig. 1), only partly flooded with mare, offers a unique opportunity to assess the nature of impact melt deposits and address questions concerning their volume, thickness, mode of emplacement, cooling and possible differentiation. A major unknown is the thickness of impact melt sheets in lunar basins. Here we apply simple cooling theory and utilize topography data to estimate the thickness of the melt sheet on the floor of the Orientale basin.

Impact Melt in the Orientale Basin: Morphology and Topography of the Maunder Formation: The Maunder Formation lies inside the Outer Rook ring and consists of two facies, both of which have historically been interpreted as impact melt [2, 7-9]. The outer corrugated or fractured facies drapes the inner plateau and peaks of the Inner Rook Ring protrude through this facies. The inner plains facies is smooth and occupies the basin floor, exposed from place to place through the thin mare fill [11, 12]. The smooth facies occurs inside the inner depression and is characterized by marginal normal faults (down to the basin interior) and a series of large fractures and polygonal cracks (Fig. 2). Most workers interpret the corrugated facies as being impact melt mixed with breccia clasts, and the smooth facies as a more pure impact melt [8-10]. M^3 data on the mineralogy of the Maunder Formation [12, 13] indicate that the upper surface of the plains facies is largely anorthositic in nature. M^3 [12, 13] and Kaguya [14] data of the Orientale region have detected no evidence for the presence of subcrustal mafic mantle material in the Orientale basin deposits. Crustal thickness below the center of the Orientale basis is estimated to be ~10 km [15]. LOLA data reveal the altimetry of the basin in detail [16] and show that the inner depression (Fig. 1) lies at an average elevation of about 2 km below the corrugated facies that occupies the Inner Rook plateau [17]. These basic data permit us to assess the original thickness of the impact melt sheet and the possibility of its differentiation.

Estimates of Melt Sheet Thickness from Topographic Relationships: A pond of liquid magma emplaced at an absolute temperature T_e first solidifies and then cools to the ambient temperature T_a. On solidification its density increases by ~10%. As it cools, its density increases further. The volumetric coefficient of thermal expansion for silicate rocks, $\alpha = -(1/v)(dv/dT)$ where v is volume and T is absolute temperature, is ~3 × 10^{-5} K^{-1} [18]. Since the volume v is inversely proportional to the density ρ for a fixed mass of lava, this implies that α is also equal to $(1/\rho)(d\rho/dT)$. Thus in cooling from ~1568 K (the average of the lava liquidus, 1713 K, and solidus, 1423 K, temperatures suggested by [19]) to the average of the lunar day and night temperatures, ~240 K, we have dT = 1328 K and hence $(d\rho/\rho)$ = 3 × 10^{-5} K^{-1} × 1328 K = 0.0398, say 0.04. Thus the density increases by a further 4% as the solid cools.

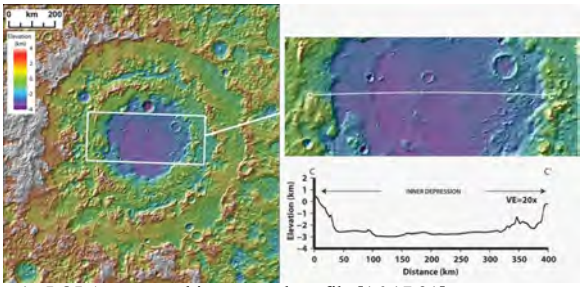

Fig. 1. LOLA topographic map and profile [16,17,21].

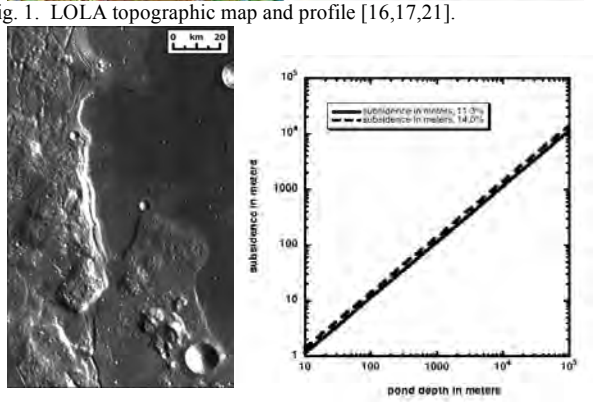

Fig. 2. (left) M^3 image of western edge of inner depression (Fig. 1).
Fig. 3. (right) Melt pond subsidence versus melt sheet thickness.

In the simple case, the total density increase, and hence the corresponding volume decrease, is ~14%. This is accommodated by both vertical subsidence and lateral shrinkage; if the linear contraction is the same in all three directions the depth decrease will be one third of this, ~4.7%, and the surface area decrease will be two thirds of this, i.e. an area change of ~9.3%. In the more realistic case, the pond cools at all of its boundaries -

with no atmosphere, the surface cools only by radiation. Plates of cooled lava form and initially founder into the liquid beneath, settling toward the base of the pond and probably being partially re-melted as they sink. At some stage foundering stops and a stable crust forms. Evidence from the drilling of the Kilauea Iki lava lake after the 1952 eruption [20] confirms that the stable crust forms well before the mean temperature of most of the depth of the pond has decreased close to the solidus. By definition a solid crust must be at the solidus temperature or lower, so it will already have effectively undergone its 10% shrinkage on solidification. As long as liquid lava does not squeeze up to completely fill fractures in this crust as it cools, it will exhibit only the consequences of the subsequent 4% volume change as it cools to ambient. One third of this volume change will be by vertical shrinkage and two thirds, i.e. ~2.7%, will be the surface area change. One test of these ideas, therefore, is to look for what would likely be polygonal fractures or depressions on the pond surface occupying 2.7% of the surface area.

The liquid magma beneath the stable crust will undergo both the 10% density increase on solidification and the 4% change on subsequent cooling. Essentially all of the 10% will be exhibited as vertical subsidence because the freezing takes place progressively. If no pore- or fracture-space is generated during the subsequent solid cooling, so will all of the 4%. However, if fractures can be supported, it is possible that up to two thirds of the 4% could be accommodated in this way leaving ~1.3% to be taken up by subsidence. We therefore expect the pond depth to decrease by between 11.3 and 14%. Note that this assumes that the initial surface crust represents only a very small fraction of the total pond volume and so does not influence this part of the calculation - this seems to be a reasonable assumption. Fig. 3 shows the subsidence expected as a function of thickness using the 11.3 and 14% limits.

Therefore, this theoretical framework provides the ability to predict: 1) the total thickness of the melt sheet on the basis of the general topographic subsidence observed (Fig. 1), and 2) the nature of the cooling of the upper thermal boundary layer on the basis of the detailed surface topography and slopes. We now proceed to assess these two aspects.

Analysis of Nature of Subsidence and Implications for Thickness of Melt Sheet: On the basis of LOLA altimetry [21] of the floor of Orientale [16, 17] (Fig. 1), the prominent topography of the interior is seen to be composed of the the Inner Rook plateau, and the inner depression, separated abruptly by the margin of the inner depression (Fig. 1, 2). Among the sources of immediate post-basin-collapse topography is general thermal equilibration of heat: 1) imparted to the substrate by the impact [22], of which impact melt is a significant part, and 2) caused by uplift of deep lithospheric isotherms during collapse, both of which are predicted to lead to thermal subsidence [22]. Deconvolution of this combined topographic signal requires further theoretical and modeling assessments; here, because the thickness of the melt sheet is so poorly known, we assume as an end-member that all of the observed topographic subsidence (Fig. 1) is due to cooling of the melt sheet. Analysis of the broad topography shows that the the inner depression is separated from the Inner Rook plateau by an average value of ~2 km (Fig. 1) and we adopt this as representing the regional thermal subsidence. In summary, on the basis of LOLA topography (Fig. 1) and basic cooling models (Fig. 3), we interpret the melt sheet to have had a maximum thickness of ~20-25 km.

Conclusions: Topographic relations in the Orientale basin are consistent with a maximum of approximately 20-25 km depth for the impact melt lake that ponded and cooled in the inner ~320 km diameter depression of the Orientale basin (Fig. 1). Even if the actual depth is only half of this maximum estimate, such cooling melt lakes are larger in volume than the largest terrestrial water lakes and seas, and greater in thickness and size than the most massive layered igneous intrusions found on Earth (e.g., Bushveld, 66,000 km^2; Dufek, 50,000 km^2). They cool and solidify from rapid surface heat loss (radiation) and relatively slower axisymmetric conduction to the sides and floor of the lake. In all cases, Skaergard-like solidification involving differentiation producing cumulates and layered igneous successions are predicted. The formation of these layered and differentiated melt lake deposits provides new insight into possible sources of igneous-appearing clasts in lunar breccias; many "highland igneous rocks" may be products of this impact melt lake sequence.

References: 1. Melosh, *Impact Cratering: A Geologic Process*, 1989; 2. Spudis, *Geology of Multi-Ring Basins*, 1993; 3. Cintala and Grieve, *MAPS* 33, 889, 1998; 4. Grieve and Cintala, *Adv. Space Res.* 20, 1551, 1997; 5. Collins et al. *Icarus* 157, 24, 2002; 6. Ivanov, *Solar Sys. Res.* 39, 381 2005; 7. Head and Wilson, *G&CA* 56, 2155, 1992; 8. Head, *The Moon* 11, 327, 1974; 9. Howard et al., *RGSP* 12, 39, 1974; 10. McCauley, *PEPI* 15, 220, 1977; 11. Whitten et al., *LPSC* 41 1841, 2010; 12. Head, *LPSC* 41 1030, 2010; 13. Pieters et al. *LPSC* 40 2052, 2009; 14. Yamamoto et al., *Nature Geosci.* 3, 533, 2010; 15. Hikida and Wieczorek, *Icarus*, 192, 150, 2007; 16. Dickson et al. *LPSC* 41, 1031, 2010; 17. Head et al., in preparation, 2011; 18. Turcotte and Schubert, *Geodynamics*, 2002; 19. Williams et al., *JGR* 105, 20189, 2000; Hardee, *JVGR* 7, 211, 1980; 21. Smith et al. *GRL*, doi: 10.1029/2010GL043751 2010; 22. Bratt et al, *JGR* 90, 12,415 1985.